Title	Tomographic Reconstruction of Uniformly Redundant Penumbral Array Camera
Author(s)	Nozaki, Shinya; Noguchi, Kentaro; Chen, Yen W.
Citation	Plasma and Fusion Research, 2: S1123-1-S1123-4
Issue Date	2007
URL	http://hdl.handle.net/20.500.12000/46089
Rights	The Japan Society of Plasma Science and Nuclear Fusion Research

Tomographic Reconstruction of Uniformly Redundant Penumbral Array Camera

Shinya NOZAKI, Kentaro NOGUCHI and Yen W. CHEN[1)]

Okinawa National College of Technology, Nago, Okinawa 905-2192 Japan

[1)]*Ritsumeikan University, Kusatsu, Shiga 525-8577, Japan*

(Received 4 December 2006 / Accepted 17 June 2007)

Penumbral imaging is a powerful imaging technique for radiations with long mean-free path. Since the reconstruction is based on deconvolution, the technique is sensitive to noise contained in penumbral images. Uniformly redundant penumbral array (URPA) technique can improve the SN ratio of penumbral images. In URPA, the penumbral apertures are arranged in m-sequence. In the reconstruction process from the coded data, penumbral image is obtained by correlation to decoding operator. The reconstructed image can be obtained by use of the Wiener filter. In this article, the three-dimensional reconstruction of the URPA and its tomographic resolution are stated.

Keywords: penumbral imaging, coded aperture imaging, m-sequence, uniformly redundant penumbral array (URPA), tomographic resolution

DOI: 10.1585/pfr.2.S1123

1. Inroduction

Penumbral imaging is a technique which uses the fact that spatial information can be recovered from the shadow or penumbra that an unknown source casts through a simple large circular aperture [1]. Since such an aperture can be "drilled" through a substrate of almost any thickness, the technique can be easily applied to highly penetrating radiation such as neutrons and γ rays. To date, the penumbral imaging technique has been successfully applied to image the high-energy x rays [1, 2], α particle, protons, and neutrons [3, 4] in laser fusion experiments. The limitation of the penumbral imaging is that the straightforward deconvolution is very sensitive to noise contained in the penumbral image [5, 6]. One of the other x-ray imaging techniques is Uniformly Redundant Array (URA) camera [7, 8]. The URA has multi pinhole apertures arranged in m-sequence. An advantage of the URA is that the S/N on the detector can be significantly improved and perfect two-dimensional reconstruction can be obtained by the use of the decoding operator.

In our previous work, uniformly redundant penumbral array (URPA) camera has been proposed to increase the SN ratio of the penumbral image, which combines the advantages of URA to the penumbral imaging [9]. In URPA, multi penumbral apertures arranged in m-sequence are used instead of single penumbral aperture. The URPA can obtain tomographic resolution because different depths in the object cast shadows with different sizes. From the advantage of the URPA, it can obtain three-dimensional reconstruction of compressed core from only viewing direction.

author's e-mail: nozaki@okinawa-ct.ac.jp

In this article, the tomographic reconstruction of the URPA is proposed and tomographic resolution is evaluated with computer simulations.

2. Penumbral Imaging

The basic concept of the penumbral imaging technique is shown in Fig. 1. The encoded image consists of a uniformly bright region surrounded by a penumbra (hatched region). Information on the source is encoded in this penumbra. The encoded image (P) can be given by

$$P(x,y) = \iint A(x,y,x',y') \cdot O(x',y')\mathrm{d}x'\mathrm{d}y', \qquad (1)$$

where $A(x,y,x',y')$ is a point spread function (PSF) of the aperture, $O(x,y)$ is a function describing the source, respectively. If the PSF of the aperture is isoplanar (space invariant), the penumbral image (P) can be written as a convolution of the source function (O) and the PSF (A) as:

$$P(x,y) = \iint A(x-x',y-y') \cdot O(x',y')\mathrm{d}x'\mathrm{d}y'. \qquad (2)$$

Thus given $P(x,y)$ and $A(x,y)$, the source image $O(x,y)$ can be reconstructed by deconvolution. Usually a Wiener filter is used for the deconvolution. In some cases, the reconstructed image can be obtained with $P(x,y)$ alone [5]. If the S/N of the penumbral image is low, the reconstructed image cannot be obtained from penumbral image since the Wiener filter is sensitive to the noise. In our previous work, heuristic method is very useful to low S/N and applied to real laser fusion experiments [6]. But since this method is based on iterative algorithm, it takes computation time.

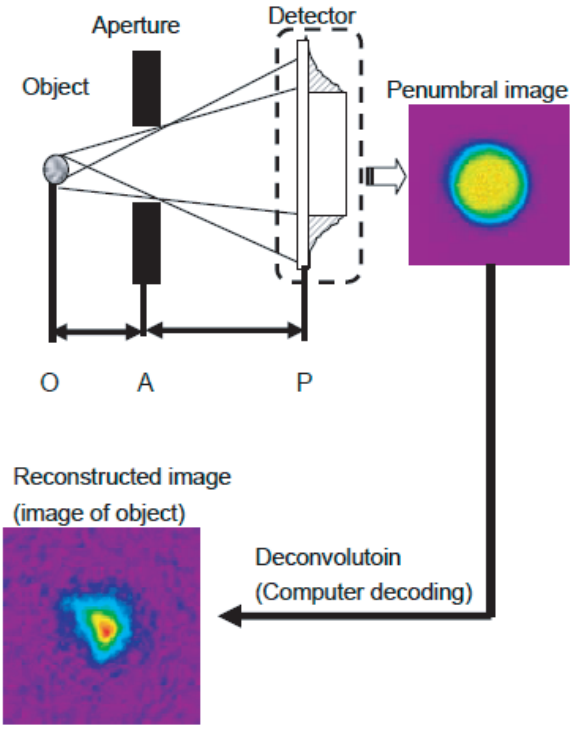

Fig. 1 The structure of the penumbral camera and the reconstruction process.

3. Uniformly Redundant Array Camera

A URA is one of the coded aperture imaging. The basic concept of the URA is shown in Fig. 2. The aperture of the camera has multi-pinhole arranged in m-sequence with an array of $r \times s$. Therefore the coded image is recorded on the detector. By using the coded image, the reconstruction can be obtained with computer decoding. If the objects is a planar (two-dimensional) object parallel to the aperture, the encoded image C is given by a correlation between O and A [8]. That is, we have

$$\begin{aligned} C(k,l) &= O * A \\ &= \sum_i \sum_j O(i,j) \\ &\quad \cdot A(\mathrm{mod}\,[i+k,r], \mathrm{mod}\,[j+l,s]), \end{aligned} \tag{3}$$

where $*$ describes correlation, O is an object image, A is the encoding operator describing the aperture function. A reconstruction can be obtained by correlating the encoded image C with a decoding operator G as

$$\begin{aligned} \hat{O}(i,j) &= C * G \\ &= \sum_k \sum_l C(k,l) \\ &\quad \cdot G(\mathrm{mod}\,[k+i,r], \mathrm{mod}\,[l+j,s]) \\ &= (O * A) * G = O * (A * G). \end{aligned} \tag{4}$$

In order to obtain perfect reconstruction, $A*G$ must be a delta function, which means that the decoding operator G must satisfy with $A*G = A$. The decoding operator G can

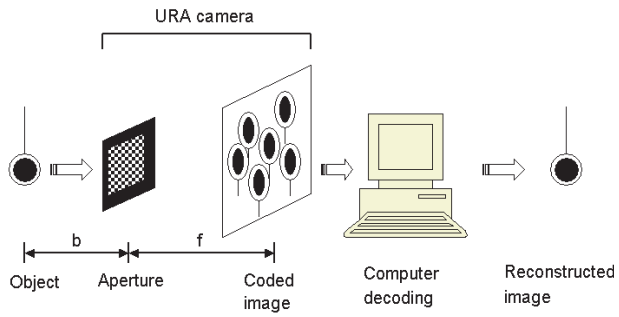

Fig. 2 The basic concept of URA imaging. The reconstructed image can be obtained from the coded image with computer decoding.

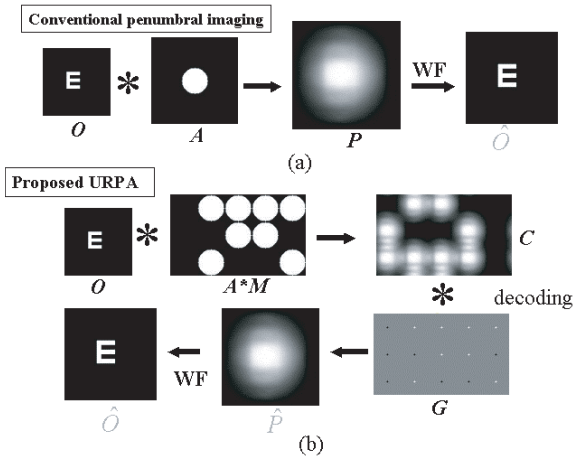

Fig. 3 The basic concept of URPA, (a) conventional penumbral imaging, (b) URPA, the S/N ratio of the decoded penumbral image is improved due to the multi-penumbral array aperture.

be selected as

$$\begin{aligned} G(i,j) &= 1 \quad if \quad A(i,j) = 1, \\ G(i,j) &= -1 \quad if \quad A(i,j) = 0. \end{aligned} \tag{5}$$

From Eq. (5), the delta function $A * G$ is given as [9]

$$A * G = \begin{cases} (r \times s + 1)/2, \mathrm{mod}\,(i,r) \\ \qquad = 0 \text{ and } \mathrm{mod}\,(j,s) = 0 \\ 0, \quad otherwise. \end{cases} \tag{6}$$

Therefore, a perfect reconstruction can be obtained with $(r \times s + 1)/2$ times flux using G as the decoding operator.

4. Uniformly Redundant Penumbral Array

The basic concept of the URPA is shown in Fig. 3. In URPA, multi-penumbral apertures are used instead of single aperture, which are arranged in m-sequence. The image (C) obtained on the detector is a coded penumbral image. The reconstruction process consists of two steps: The first step is to use a decoding operator to obtain the

real penumbral image and the second step is a deconvolution process. In the second step, a Wiener filter is used to reconstruct the source image.

Compared with signal-to-ratio (S/N) of the conventional penumbral image shown in Fig. 3 (a), the S/N of the decoded penumbral image shown in Fig. 3 (b) is significantly improved [9].

5. Tomographic Reconstruction by the URPA

The basic concept of tomographic imaging with URPA is shown in Fig. 4. Source distant to the detector cast smaller aperture shadows than closer sources. The size of the shadow depends on the distance to the point, while the location of the shadow depends on the lateral displacement of the point. By correlating the recorded image with decoding patterns of different sizes, images of the source distribution at different depths can be retrieved.

The concept of the tomographic imaging can be expressed in mathematical terms. Let $C(x, y)$ be an encoded image at position (x, y) on the detector, $O_z(x, y)$ be the distribution in a plane parallel to the aperture and a distance z from it, $M_z(x, y)$ be a two-dimensional m-sequence of the aperture, and let $A_z(x, y)$ be the appropriately magnified version of the aperture for the distance z. Since $O_z(x, y)$, $M_z(x, y)$, and $A_z(x, y)$ depend on the magnification (distance z), they can be also expressed as a function of z, respectively. We have the recorded image which is a sum of the correlation of each object plane with an aperture pattern of appropriate magnification. Therefore we have as follows:

$$C(x, y) = \sum_z [O_z(x, y) * A_z(x, y) * M_z(x, y)]\cdot \quad (7)$$

To retrieve $P(x, y)(= O_z(x, y) * A_z(x, y))$ including the *z-th* plane information $O_z(x, y)$, a decoding operator $G_z(x, y)$ is correlated. That is, we have

$$\begin{aligned}\hat{P}_z(x, y) &= C(x, y) * G_z(x, y) \\ &= \sum_z{}' [P'_z(x, y) * M'_z(x, y)] * G_z(x, y), \end{aligned} \quad (8)$$

where, if $z = z'$, $M_z(x, y) * G_z(x, y)$ is a delta function. On the other hand, $M_z(x, y) * G_z(x, y)$ is not the delta function if $z \neq z'$. Therefore Eq. (8) becomes

$$\begin{aligned}\hat{P}_z(x, y) &= \sum_z{}' [P'_z(x, y) * M'_z(x, y)] * G_z(x, y) \\ &= P_z(x, y) \\ &\quad + \sum_{z \neq z'} [P'_z(x, y) * M'_z(x, y) * G_z(x, y)] \\ &= P_z(x, y) + \Delta P_z. \end{aligned} \quad (9)$$

If the second term is 0, the *z-th* perfect penumbral image is obtained. But the second term is not 0 since $M'_z(x, y) * G_z(x, y)$ is not the delta function in the case of $z \neq z'$. Since an artifact appears in each reconstructed image, the tomographic resolution of the URPA camera is reduced.

6. Computer Simulation for the Verification of the Proposed Method

A computer simulation was carried out to evaluate the tomographic resolution of the URPA. An arrangement of the computer simulation is shown in Fig. 5. The distance between the source point and aperture is Z_0. The reconstructed image is obtained with Z. If the tomographic resolution is very high, the source point can be obtained in the case of only Z equals to Z_0.

The reconstructed images are shown in Fig. 6. When the Z equals to Z_0, the source point can be clearly observed.

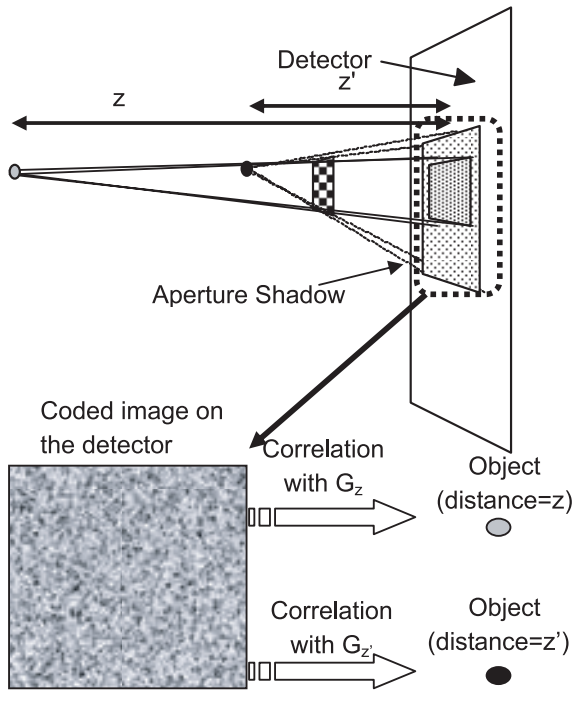

Fig. 4 The basic concept of URPA tomographic imaging. Each reconstruction can be obtained by using the decoding operator.

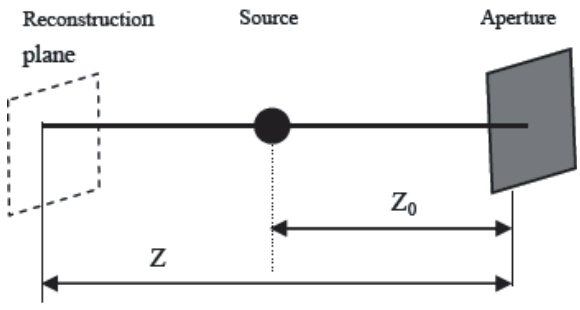

Fig. 5 An arrangement of the computer simulation for evaluating the tomographic resolution of the URPA.

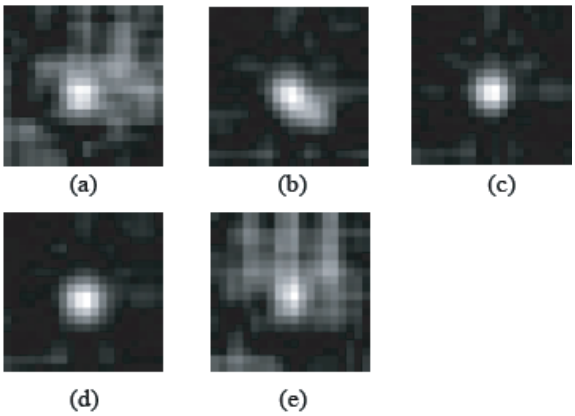

Fig. 6 The reconstructed images. (a) $Z/Z_0 = 0.9$ (b) $Z/Z_0 = 0.99$ (c) $Z/Z_0 = 1.0$ (d) $Z/Z_0 = 1.01$ (e) $Z/Z_0 = 1.1$.

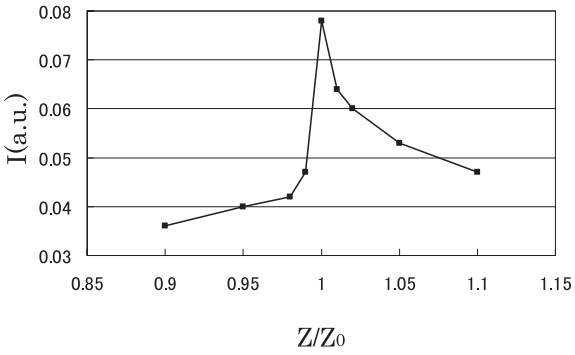

Fig. 7 The depth of the point spread function of the URPA.

When Z does not equal to Z_0, the source point is gradually blurred. Therefore, it can be seen that the URPA has the tomographic resolution of viewing direction.

The depth point spread function of the URPA is shown in Fig. 7. It can be seen that intensity of $Z/Z_0 < 1$ is smaller than that of $Z/Z_0 > 1$ due to the magnification of the camera. The reconstruction of the large magnification is better in quality than that of smaller one. The intensity of $Z/Z_0 = 1$ is 0.078. Compared with URA (multi-pinhole) method [8], the intensity is small. But the URPA can obtain the high SN ratio image on the detector because the aperture of the URPA is larger than that of the URA [9]. Therefore the URPA is applicable for highly penetrating radiations or low intensity radiations.

7. Conclusion

In this article, the tomographic reconstruction of the URPA was proposed. From the computer simulation, it can be seen that tomographic reconstruction can be obtained.

To apply the camera to future laser fusion experiments, more study of improving the tomographic resolution is needed.

[1] K.A. Nugent and B-Luther-Davis, Opt. Commun. **49**, 818 (1984).
[2] D. Ress, R.A. Lerche, R.J. Ellis, S.M. Lane and K.A. Nugent, Science **241**, 956 (1988).
[3] Y.-W. Chen *et al.*, IEICE Trans. Electron **Vol. E78-C**, 1787 (1995).
[4] Y.-W. Chen, Z. Nakao, I. Tamura, IEICE Trans. Electron **Vol. E80-C**, 346 (1997).
[5] S. Nozaki *et al*., Rev. Sci. Instrum. **74**. 2240 (2003).
[6] S. Nozaki *et al*., Rev. Sci. Instrum. **73**. 3198 (2002).
[7] Y.-W Chen and K. Kishimoto, Rev. Sci. Instrum. **74**, 2232 (2003).
[8] Y.-W Chen *et al*., Opt. Commun. **71**, 249 (1989).
[9] Y.-W Chen *et al*., Rev. Sci. Instrum. **75**, 4017 (2004).